

A three-dimensional sorting reliability algorithm for coastline deformation monitoring, using interferometric data.

J v Genderen and M Marghany¹

Institute of Geospatial Science and Technology (INSTeG)
Universiti Teknologi Malaysia
81310 UTM, Skudai, Johor Bahru, Malaysia

Email:maged@utm.com

Abstract. The paper focusses on three-dimensional (3-D) coastline deformation using interferometric synthetic aperture radar data (InSAR). Conventional InSAR procedures were implemented on three repeat passes of ENVISAT ASAR data. Furthermore, the three-dimensional sorting reliabilities algorithm (3D-SRA) were implemented with the phase unwrapping technique. Subsequently, the 3D-SRA was used to eliminate the phase decorrelation impact from the interferograms. The study showed that the performance of the InSAR method using the 3D-SRA algorithm, is better than the conventional InSAR procedure. In conclusion, the integration of the 3D-SRA, together with phase unwrapping, can produce accurate 3-D coastline deformation information.

1. Introduction

Coastal erosion is a destructive and often a serious natural disaster. Coastal erosion has both direct and indirect consequences for coastal communities, resulting in abandonment of beachfront properties, and modification of coastal infrastructure and, in extreme cases, causing loss of life. At present, because of sea-level rise, and climate change (such as an increase in storm surges, hurricanes, etc) there is worldwide increase in coastal erosion, usually apparent in the progressive retreat of backshore cliffs, dunes, spits, and the concomitant landward displacement of the shoreline [1-3]. In this regard, coastal erosion requires standard procedures for monitoring, modelling, and mapping [4].

InSAR has shown that it can provide DEMs with 1-10 cm accuracy, which can be improved to millimetre level by Differential synthetic aperture radar Interferometry (DInSAR) [5-8]. In this regard, sub-centimeter target displacements can be detected using DInSAR along the sensor-target direction [1,7,9]. In comparison with other conventional techniques such as levelling, and GPS, DInSAR provides valuable information about target displacement, over large areas, at a relatively low cost [10-11]. In fact, conventional methods are time consuming and they are required some control points [5,12]. DInSAR has many other applications as well, such as monitoring geophysical natural hazards, for instance earthquakes, volcanoes and landslides, also in engineering, in particular recording of subsidence and structural stability. Over time-spans of days to years, InSAR can detect the centimetre-scale of deformation changes [13]. Furthermore, the precision of DEMs from the InSAR technique is quite high, compared to conventional remote sensing methods. In many countries, the 90 m SRTM data, or the 30 m. DEM data from ASTER are the main sources of DEMs [9,14]. The main contribution of this study is to implement three three-dimensional phase unwrapping algorithms with the InSAR technique. Three hypotheses examined in this paper are: (i) three three-dimensional phase unwrapping algorithms can be used as a filtering technique to reduce noise in the phase

¹ To whom any correspondence should be addressed.



unwrapping [3]; (ii) 3-D shoreline reconstruction can be produced using satisfactory phase unwrapping by involving the three three-dimensional phase unwrapping algorithm; and (iii) high accuracy of deformation rate can be estimated by using the new technique.

2. DEM reconstruction using a three-dimensional sorting reliabilities algorithm (3D-SRA)

Hussein et al., [15] have proposed a new algorithm for three-dimensional phase unwrapping. The algorithm is called a three-dimensional sorting reliability algorithm (3D-SRA). Marghany [16] has implemented this for 3-D coastal erosion modelling. The quality of each edge of phase unwrapping is a function of the connection of two voxels in 3-D Cartesian axis e.g. , x , y , z . This involves carrying out the unwrapping path from the high quality voxels to the lower quality voxels [17]. In addition, following a discrete path, the 3D-SRA algorithm unwraps the phase volume which is significant to determine the 3-D volume change rate of the shoreline. In this regard, the voxels connects the highest reliable edges that are unwrapped first with border surfaces. Consistent with Hussein et al., [15], the reliability value of an edge that connects a border voxel with another voxel in the phase volume is set to zero. Let E_x , E_y , and N are the horizontal, vertical, and normal second differences, respectively which are given by

$$E_x(i, j, k) = \gamma[\phi(i-1, j, k) - \phi(i, j, k)] - \gamma[\phi(i, j, k) - \phi(i+1, j, k)], \quad (1)$$

$$E_y(i, j, k) = \gamma[\phi(i, j-1, k) - \phi(i, j, k)] - \gamma[\phi(i, j, k) - \phi(i, j+1, k)], \quad (2)$$

$$N(i, j, k) = \gamma[\phi(i, j, k-1) - \phi(i, j, k)] - \gamma[\phi(i, j, k) - \phi(i, j, k+1)], \quad (3)$$

where i, j, k are the neighbours' indices of the voxel in $3 \times 3 \times 3$ cube, and γ defines a wrapping operator that wraps all values of its argument in the range $[-\pi, \pi]$. Using the sum of equations 1 to 3, the second difference quality map Q can be obtained [18]

$$Q_{i,j,k} = \sqrt{E_x^2(i, j, k) + E_y^2(i, j, k) + N^2(i, j, k)} \quad (4)$$

The unwrapping path is performed based on equation 10 where entirely the edges are stored in a 3D array and sorted with their edge quality values [18,20]. Further, unwrapping a voxel or a group of voxels concerning another group may require the addition or subtraction of multiples of 2π [16].

3. Results and discussions

Figure 1 shows the ENVISAT ASAR data sets of 5 March 2003 (SLC-1), and January 25, 2011, (SLC-3) of Wide Swath Mode (WSM) (Figure 1) used for InSAR data. processing. They are acquired from ascending (Track: 226, orbit: 5290), and descending (Track 420, Orbit 4655), respectively.

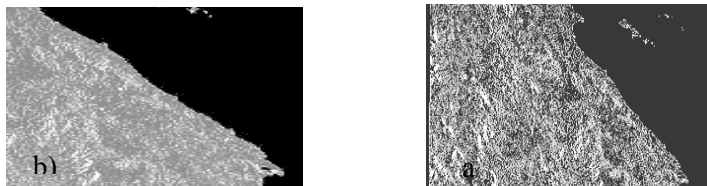


Figure 1. ENVISAT ASAR data used in this study
(a) 5 March 2003; and (b) January 25 2011.

Clearly, there is huge differences between InSAR DEM and DEM generated from in situ measurements with 9 m differences while in situ measurements agree with the DEM produced from

the topographic map to within 1.3 m differences (Figure 2). This is because the impact of decorrelation. This result confirms the previous work done by Marghany [1] and [16]. Figure 3 shows discontinuities interferogram fringes, generated using conventional InSAR procedures. This could have occurred because of the high decorrelation. [1,16].

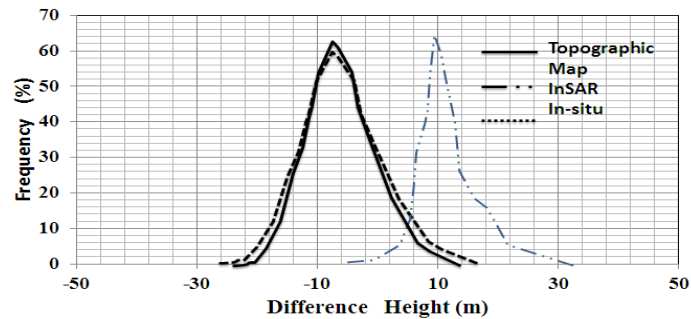


Figure 2. Height differences between DEM generated from InSAR, topographic map and in situ measurements.

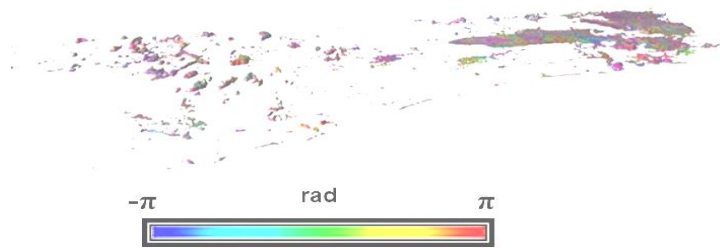


Figure 3. Interferogram generated from InSAR data.

Figure 4 shows the interferogram produced by using the three-dimensional sorting reliabilities algorithm 3-DSR. Clearly, the 3DSR algorithm for phase unwrapping produced clear fringe cycles which indicate critical erosion of -3.5 m/year. This study confirms the work done by Hussein et al., [15,17]. The three-dimensional sorting reliabilities algorithm provides an excellent 3-D phase unwrapping which leads to high quality 3-D coastline reconstruction. This contributes to a high quality map. Indeed, the 3-DSR algorithm is guided by including the maximum gradient quality maps. Therefore, quality maps guide the unwrapping path through a noisy region so that the interferogram patterns are in completing cycles as compared to the conventional InSAR interferogram.

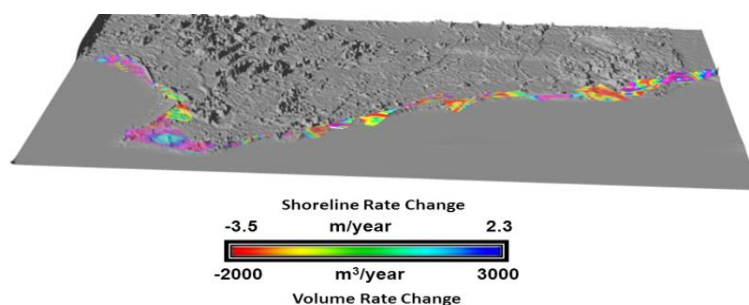


Figure 4. Fringe interferometry generated by a three-dimensional sorting reliabilities algorithm.

4. Conclusions

The paper has illustrated the use of InSAR phase unwrapping using the three-dimensional sorting reliabilities algorithm (3-DSR). The main purpose of this technique is to solve the decorrelation problem that is a critical issue with InSAR techniques. In addition, three-dimensional (3-D) coastline deformation from interferometry synthetic aperture radar (InSAR) is estimated. In conclusion, the 3-DSR algorithm can be used to solve the problem of decorrelation and produced accurate 3-D coastline deformation using ENVISAT ASAR data.

References

- [1] Marghany M 2013 *Acta Geoph* **61** 493
- [2] Marghany M, Hashim M and Cracknell A.P 2011 *Env. Earth Sci.* **64** 1189
- [3] Zhou Y, LI D and Genderen J L 1999 *Int. Soc. for Opt. and Phot* **5** 208
- [4] Marghany M 2012 *Comp. Sci. and Its Appl. – ICCSA 2012 Lec. Not in Comp. Sci.* **7335** 446
- [5] Aiazzi B, Baronti S, Bianchini M, Mori A and Alparone L 2005 *EUR. J. on App. Signal Proc.* **20** 3230
- [6] Gens R and Genderen J L 1996 *Int. J. of Remote Sens.* **17** 1835
- [7] Hangdog F, Kazhong D, Chengyu J, Chuanguang Z and Jiqun X 2011 *Min. Sci. and Tech. (China)*, **21** 872
- [8] Ferretti A, Prati C and Rocca F 2001 *Il Nuovo cimento della Società italiana di fisica. C. Geophysics and space phys.* **24** 176
- [9] Zebker H A, Rosen P A, and Hensley S 1997 *J. of Geophy. Res.* **102** 7563
- [10] Baselice F, Ferraioli G and Pascazio V 2009 *IEEE Geos. Remote Sensing* **6** 257
- [11] Ferraioli G, Pascazio V and Schirinzi G 2004 *IEEE Geos. Rem. Sens. Let.* **2** 70
- [12] Massonnet D and Feigl K L 1998 *Rev. Geoph.* **36** 441–500
- [13] Guariglia A, Buonamassa A, Losurdo A, Saladino R, Trivigno M.L, Zaccagnino A and Colangelo A 2006 *Ann. of Geophy.* **49** 304
- [14] Nizalapur V, Madugundu R and Shekhar C J 2011 *J. App. Remote Sens.* **5** 1-059501-6
- [15] Hussein S A, Gdeist M, Burton D and Lalor M 2005 *Proc. SPIE* **5856** 40
- [16] Marghany M. 2013 *Comp. Sci. and Its Appl. – ICCSA 2013 Lec. Not in Comp. Sci.* **7972**610
- [17] Hussein S A, Munther A, Gdeisat M, David R, Michael J, Lalor F L, and Moore C 2007 *Appl. Opt.* **46** 6635